Multifunctional P450 Monooxygenase CftA Diversifies the Clifednamide Pool Through Tandem C–H Bond Activations

Jinping Yang,[†] Yunci Qi,[‡] Joshua A. V. Blodgett,[‡] * Timothy A. Wencewicz[†]*

[†]Department of Chemistry, Washington University in St. Louis, One Brookings Drive, St. Louis, MO, 63130, USA.

[‡]Department of Biology, Washington University in St. Louis, One Brookings Drive, St. Louis, MO, 63130, USA.

Polycyclic tetramate macrolactams (PTMs) are a class of structurally complex hybrid polyketidenonribosomal peptide (PK-NRP) natural products produced by diverse bacteria. Several PTMs display pharmaceutically-interesting bioactivities, and the early stages of PTM biosynthesis involving polyketide synthase (PKS) and non-ribosomal peptide synthetase (NRPS) enzymology are well-studied. However, the timing and mechanisms of post PKS-NRPS oxidations by P450 monooxygenases encoded in PTM biosynthetic gene clusters (BGCs) remain poorly characterized. Here we demonstrate that CftA, encoded in clifednamide-type PTM BGCs, is a multifunctional P450 monooxygenase capable of converting the C29-C30 ethyl side chain of ikarugamycin to either a C29-C30 methyl ketone or a C29-C30 hydroxymethyl ketone through C-H bond activation, resulting in the formation of clifednamide A or clifednamide C, respectively. We also report the complete structure of clifednamide C solved via multi-dimensional NMR (COSY, HSQC, HMBC, NOESY, and TOCSY) using material purified from an engineered Streptomyces strain optimized for production. Finally, the in vitro reconstitution of recombinant CftA catalytic activity revealed the oxidation cascade for sequential conversion of ikarugamycin to clifednamide A and clifednamide C. Our findings confirm prior genetics-based predictions on the origins of clifednamide complexity via P450s encoded in PTM BGCs, and place CftA into growing group of multifunctional P450s that tailor PTM natural products through late-stage regioselective C-H bond activation.

Polycyclic tetramate macrolactams (PTMs) are a class of microbial secondary metabolites with a broad-spectrum of bioactivities including antibacterial, antifungal, and antitumor properties. PTM core structures incorporate characteristic ornithine-derived tetramate moieties and macrolactam scaffolds that are often fused to polycyclic carbon-based ring systems. PTM polycycle patterns vary by compound, with combamide (5-5), heat-stable antifungal factor (HSAF) (5-5-6), and ikarugamycin (5-6-5) as representative PTM scaffold architectures (Figure 1 and S1). Despite the diversity of PTM structures, PTM BGCs share a high degree of similarity among the encoded biosynthetic enzymes (Figure 1; Table S1-S4). Critical for their biosynthesis, these BGCs encode a hallmark iterative polyketide synthetase-nonribosomal peptide synthetase (PKS-NRPS, IkaA/FtdB) hybrid enzyme responsible for producing the universal polyene tetramate precursor, lysobacterene A (Figure S2). This polyene is then intramolecularly crosslinked to form diverse ring systems by phytoene-dehydrogenase and alcohol-dehydrogenase type redox enzymes in characterized reaction cascades.

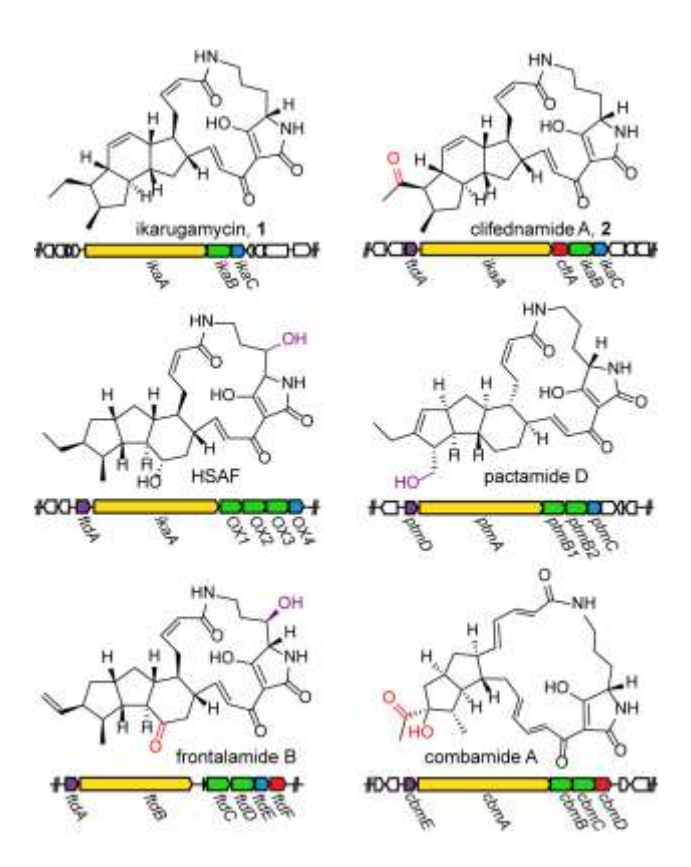


Figure 1. Chemical structures and BGCs for structurally diverse PTM analogues, ikarugamycin (1),³ clifednamide A (2),⁸ HSAF,^{5,6} pactamide,⁹ frontalamide,¹⁰ and combamide.⁴ The ORFs are colored in 'yellow' for encoding hybrid PKS-NRPS synthetases, 'green' for FAD-dependent oxidoreductases, 'blue' for Zn-dependent alcohol dehydrogenases, 'purple' for fatty acid desaturases. The genes encoding cytochrome P450 enzymes are colored in red. Genes shown in 'white' are flanking genes in known producers and have no known biosynthetic function.

In addition to the various carbocyclic ring architectures that diversify PTM scaffolds, tailoring enzymes including cytochrome P450 monooxygenases and fatty acid desaturase-family oxidases further modify and differentiate PTM congeners through C-H activation chemistry that includes hydroxylation, epoxidation, and ketone formation.^{1,4,8,10–14} The resulting oxidized analogues presumably enhance target binding and increase the water solubility of otherwise hydrophobic PTM scaffolds. Genome mining, strain engineering, and *in vivo* mutational analyses have linked

several PTM enzymes with their oxidative roles, including fatty acid hydroxylase FtdA (frontalamides),^{10,11} cytochrome P450 CbmD (combamides),⁴ and cytochrome P450 CftA (clifednamides) (Figure 1).⁸ Understanding and manipulating the late-stage oxidation of natural products is an attractive strategy to improve molecular potency, solubility, and other physiochemical properties. It also provides synthetic handles for further derivatization towards the production of semi-synthetic variants.^{15,16}

The clifednamide family of PTMs (clifednamides A–J, Figure S1) is an interesting system for the study of PTM site-selective late-stage oxidations and their structure-function consequences. 8,17-19 First discovered in 2010 in growth extracts of *Streptomyces* sp. strain JV178 isolated from Connecticut, USA soils, clifednamides have now been re-discovered in several globally-distributed Streptomyces strains. 8,17,18,20 To date, clifednamide biosynthesis has been investigated by multiple research groups using a combination of genome mining, gene deletion and synthetic biology approaches. Initial investigations by Qi and coworkers linked clifednamide production to a distinct 5-gene BGC (ftdA-ikaA-cftA-ikaBC) encoded within the genome of Streptomyces sp. strain JV178.8,21 Through mutational analyses in another producer, Streptomyces sp. strain NRRL F-6131, it was established that clifednamide A (2) and B are essentially C29 keto derivatives of ikarugamycin and butremycin, respectively, and C29 oxidation in the strain was linked to the cluster-encoded cytochrome P450 CftA. Through a series of synthetic biology inquires by the Li and Blodgett groups, 8,18 several new oxidative variants and biosynthetic intermediates of the clifednamides (clifednamides C-J) were discovered. In terms of CftA P450 enzymology, the most interesting of these new clifednamides are those having previously undiscovered C29-C30 hydroxymethyl ketone moieties – clifednamide C (compound 3; this work) and clifednamide E (Li and coworkers). 18 The formation of a C29-C30 hydroxymethyl ketone

suggests that CftA is capable of site-selective tandem C-H activation chemistry as a multifunctional P450 employed for late-stage PTM scaffold diversification.

Initial evidence for the existence of clifednamide C (3) was first obtained by members of the Blodgett group while analyzing the PTM production profile of the robust engineered clifednamide A producer (JV772). HRMS and MS/MS fragmentation mapping suggested clifednamide C (3) contains an additional ¹⁶O in the 5-6-5 polycyclic region beyond what is observed for clifednamides A (2) and B.8 JV772 was created by engineering Streptomyces sp. NRRL F-2890, a strong ikarugamycin producer, to host the cftA gene of Streptomyces sp. strain JV178 under the control of a strong constitutive promoter (PermE*)(Figure S3).8 Because the formation of both clifednamide A (2) and the new spectrometrically-detected congener clifednamide C (3) depended on the expression of cftA, it was postulated that CftA might have multiple oxidative activities (Figure 2). Fragmentation analyses suggested clifednamide C (3) might be a hydroxy or epoxide derivative of clifednamide A (2), but its structure was left unsolved. In a follow up study, workers in the Li group then heterologously reconstituted clifednamide biosynthesis in *Streptomyces* sp. strain S001 using cryptic BGC genes cloned from Kitasatospora sp. strain S023. This effort significantly expanded the number of known clifednamide pathway products to include clifednamides D-J, (leaving clifednamide C (3) structure unsolved), and importantly revealed a new clifednamide congener having a C29-C30 hydroxymethyl ketone moiety (clifednamide E). Together with the strain JV772 data, the discovery of clifednamide E further bolsters the idea that CftA might be a bifunctional P450 oxygenase, similar to other PTM-associated P450s including IkaD and CbmD. Finally, the Li group found clifednamides A, B and H are cytotoxic to certain mammalian cell lines.²² As ikarugamycin derivatives, clifednamides might act by directly inhibiting hexokinase 2 and arresting glycolysis, as postulated for other 5-6-5 PTMs including ikarugamycin (1) and caspimycins.²²

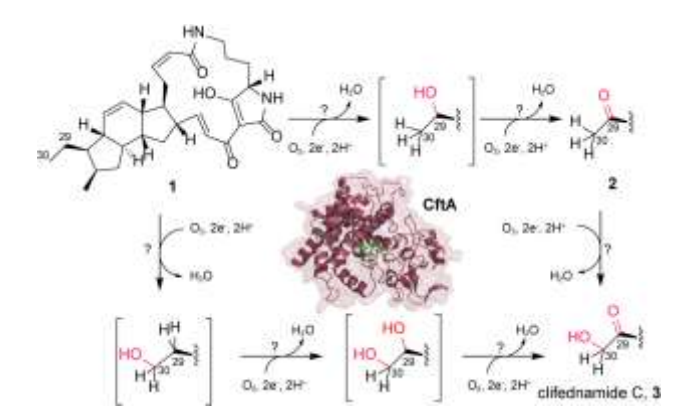


Figure 2. Proposed tandem C-H bond activation at C29–C30 showing the conversion of ikarugamycin (1) to clifednamides A (2) and C (3) catalyzed by CftA (homology model constructed using SWISS model (https://swissmodel.expasy.org/) with MycG (PDB: 5uhu) as template structure).

To further probe clifednamide PTM molecular diversity, completely elucidate the origins of their observed oxidative diversity, and enable future structure-function analyses within the family, here we report the complete structural characterization of clifednamide C (3) using 2D NMR and high-resolution MS/MS techniques. In agreement with earlier but incomplete MS/MS characterization of the compound, this revealed the presence of a hydroxymethyl ketone at C29-C30. Because prior *in vivo* genetic experiments were unable to rule out the possibility of other cellular enzymes being involved in the oxidation of ikarugamycin (1) to clifednamide C (3), we also report the *in vitro* reconstitution of P450 CftA enzymatic activity. Our findings confirm the enzyme's role in the single oxidation of C29 in ikarugamycin (1) to form clifednamide A (2), and also directly demonstrate its role in the tandem oxidation of the C29-C30 ethyl group for the ordered sequential formation of clifednamide C (3) via clifednamide A (2).

Results and Discussion

Preparative scale purification of clifednamides A (2) and C (3). Clifednamides A (2) and B were originally isolated from *Streptomyces* sp. JV178 in 2010 (Figure S3; Table S5)¹⁷ and were fully characterized by multi-dimensional NMR. However, production of these compounds by strain JV178 was sparing. To overcome compound paucity, in 2017 the Blodgett lab reported the construction of recombinant *Streptomyces* sp. strain JV772 to increase clifednamide A (2) availability. During these studies, a new congener named clifednamide C (3) was identified by mass-fragmentation as a new constitutional isomer of clifednamide B.⁸ The production of both clifednamides A (2) and C (3) depended on expression of the P450 CftA in strain JV772,⁸ which strongly suggested clifednamide C (3) could be an oxidation product of clifednamide A (2). However, the structure of clifednamide C (3) and CftA's potential role as a multifunctional oxidase remained largely uncharacterized following these studies.

We achieved preparative scale production and purification of clifednamide A (2) and C (3) from solid cultures of *Streptomyces* sp. strain JV772 (~5 mg compound in >90% purity from ~200 mg of crude concentrate from EtOAc extractions). The compounds were separated by RP-C₁₈ prep-HPLC and fractionated according to LC-MS purity analysis (Figure S4–S7). Clifednamide C (3) exhibited an earlier retention time, consistent with the proposal that it is an oxidation product of clifednamide A (2). We used multi-dimensional NMR analysis to confirm the structure of clifednamide A (2)¹⁷ and assign the structure of previously unidentified clifednamide C (3).

Structure elucidation of clifednamide C (3). Blodgett and coworkers originally reported the molecular formula of clifednamide C (3) as $C_{29}H_{36}N_2O_6$ based on HRMS analysis (m/z 509.2645 $[M+H]^+$, calculated 509.2646). The timing of product appearance in strain JV772 culture (clifednamide A (2) accumulated first, followed by clifednamide C (3) with concomitant loss of

clifednamide A (2)) and the observed 16 amu increase in molecular mass relative to clifednamide A (2), suggests that clifednamide C (3) is an oxidized product derived from clifednamide A (2). Purified clifednamide C (3) was obtained as a light pink powder, and we obtained 1D (1 H, 13 C) and 2D (COSY, TOCSY, NOESY, HSQC, HMBC) NMR spectra of this sample dissolved in DMSO- d_{6} . Using these data, we searched for key spectral changes relative to the previously reported spectral data for clifednamide A (2).

The ¹H-NMR spectrum for clifednamide C (3) showed the presence of six olefinic protons [$\delta_{\rm H}$ (ppm) 5.83 (1H, d, *J*=11.4 Hz), 5.94 (1H, dd, *J*=11.4, 11.4 Hz), 5.63 (1H, d, *J*=9.8 Hz), 5.70 (1H, d, J=9.8 Hz), 5.95 (1H, m), 7.49 (1H, d, 15.4 Hz)], which supports that all of the original olefins in clifednamide A (2) remained intact, making them unlikely sites for CftA-mediated oxidation. We also observed a new set of strongly coupled ¹H resonances with chemical shifts at ~4 ppm that appear as a set of doublets with a coupling constant (J=18.5 Hz) consistent with geminal ¹H-¹H coupling near a hydroxy group (Figure 3a). Meanwhile, the distinctive singlet at ~2 ppm corresponding to the C30 methyl group of the clifednamide A C29-C30 methyl ketone was missing. This indicated the methyl group at C30 was likely the site of additional hydroxylation in clifednamide C. HMBC supported this supposition through the observed ¹H-¹³C couplings from the ¹H's on C30 and C10 to the ketone ¹³C carbonyl of C29 (Figure 3b) and the structure of clifednamide C (3) was determined as 29-oxo-30-hydroxy-ikarugamycin. This proposed structure is consistent with the observed chemical shifts, splitting, and coupling observed by multidimensional NMR for other natural products containing hydroxymethyl ketones including pleuromutilin [4.04 ppm (qd, J=17.1, 5.4 Hz)), ²³ doxorubicin [4.70 ppm (d, J=4.1 Hz)), ²⁴ and the recently reported clifednamide E [4.13 ppm (d, J=18.5 Hz), 4.04 ppm (d, J=18.5 Hz)).¹⁸

We confirmed the relative connectivity and stereochemistry of clifednamide C (3) using a variety of ¹H-¹H and ¹H-¹³C correlation spectroscopic methods including COSY, TOCSY, NOESY, HMBC, and HSQC. The COSY and HMBC correlation patterns for clifednamide C (3) were very similar to those previously reported for clifednamide A (2) and ikarugamycin (1) indicating that these compounds share analogous polycyclic 5-6-5 fused ring systems (Figure 3b). 17 The locations of the C2-C3 and C17-C18 olefins were confirmed via COSY correlations to C4 and C16, respectively. HMBC correlations were also observed from C2-C1 and C18-C19. The double bond configurations in the macrolactam ring were assigned for C2-C3 as (Z) and C17-C18 as (E) from the proton coupling constants ($J_{2,3}=11.4$ Hz and $J_{17,18}=15.4$ Hz). Additionally, the enolform of the tetramate moiety was confirmed based on the observed ¹³C-resonance chemical shifts of 104 ppm and 196 ppm for C20 and C24, respectively. We observed strong through-space ¹H-¹H correlations in the NOESY spectrum between hydrogens on C10-C11 confirming the synorientation of the methylketone and methyl groups at C10 and C11, respectively. We also observed transannular NOESY signals confirming that ikarugamycin (1), clifednamides A (2), and C (3) share the same relative stereochemical configurations. In addition, the ECD spectra (Figure S26) for clifednamide C (3) is similar to that of ikarugamycin (1)¹⁸. Thus, the configuration of clifednamide C (3) was assigned as 5S,6R,9R,10R,11R,13R,14R,16S,23S.

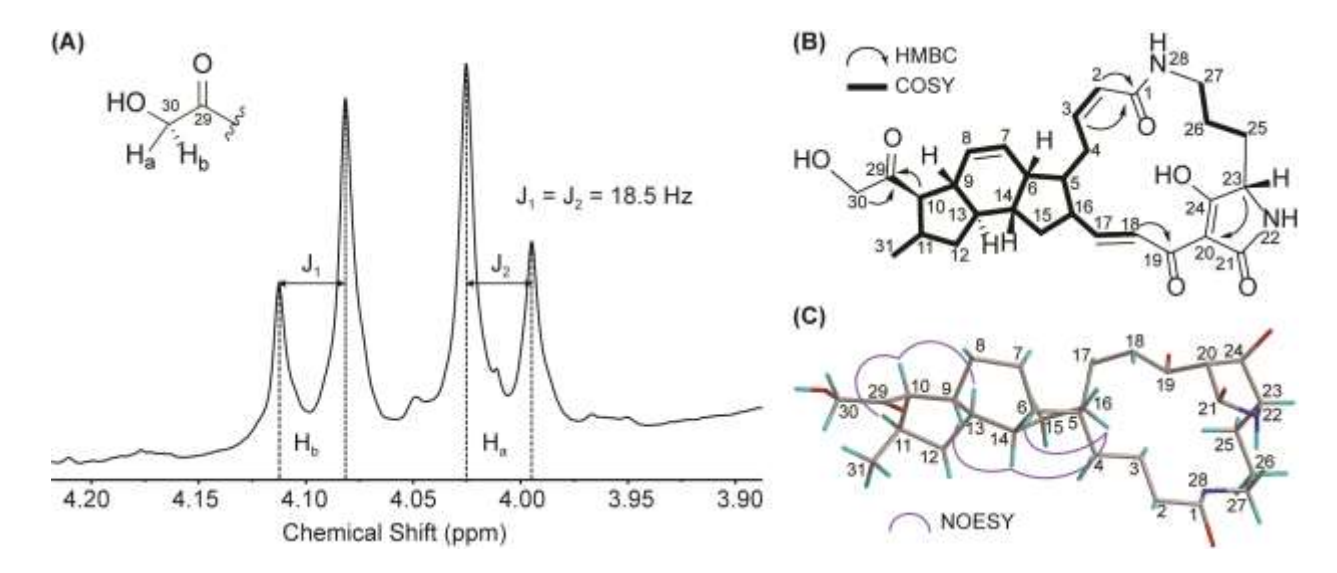


Figure 3. NMR structure elucidation of clifednamide C (3). (a) Isolated region of the 1 H NMR spectrum of clifednamide C (3) from 3.90 – 4.20 ppm showing diastereotopic methylene hydrogens appearing as doublets (J = 18.5 Hz). (b) Diagnostic resonance correlations from HMBC ($^{1}\text{H}-^{13}\text{C}$) and COSY ($^{1}\text{H}-^{1}\text{H}$) 2D NMR experiments are highlighted as arrows and extra thick bolded bonds, respectively. (c) Diagnostic resonance correlations from NOESY ($^{1}\text{H}-^{1}\text{H}$) 2D NMR experiments indicated by purple connecting curves (3D structure generated using Chem3D, CambridgeSoft).

Expression, purification, and characterization of P450 monooxygenase CftA. In light of the prior biosynthetic analysis of strain JV772 and our confirmed structural similarity of ikarugamycin (1), clifednamide A (2), and C (3), we hypothesized that the P450 monooxygenase CftA encoded in clifednamide BGCs is responsible for converting ikarugamycin (1) into clifednamides A (2) and C (3) (Figures 1 and 2). We directly tested this hypothesis through the first in vitro reconstitution of CftA catalytic activity. Leveraging the fact that there are several sequenced cftA orthologs reported in public sequence databases, we initially cloned several variants (cftA_{JV178}, cftA_{purpeofuscus}, cftA_{F-6131}, and cftA_{torulosus}) into a pET28 for protein expression with an N-terminal-His₆ affinity tag. Following attempted heterologous expression of each ortholog in E. coli BL21(DE3), these efforts

failed to achieve robust protein expression, presumably due to the high G+C content of the *cftA* genes from the originating *Streptomyces* strains. Instead, we used a codon optimization scheme to refactor the codon usage of *cftA* from *Streptomyces* sp. JV178 (Table S6-S7) to reflect more closely that of *E. coli*. This led to excellent heterologous expression of *N*-His₆-tagged CftA in *E. coli* BL21(DE3) (Figure S9a). Purification of this CftA construct via Ni-NTA affinity chromatography provided a high-quality protein sample (>90% pure by SDS-PAGE) suitable for biochemical characterization and *in vitro* reconstitution of enzyme activity.

To confirm the presence of expected spectral shifts characteristic of heme prosthetic group binding, we treated recombinant CftA with various oxidizing and reducing agents, along with ligands ikarugamycin (1), clifednamide A (2), and C (3). The optical absorbance spectra of CftA under aerobic conditions at pH 7.4 showed UV absorbance bands (major Soret band located at 425 nm, and alpha and beta absorption bands at 560 and 510 nm respectively) consistent with the presence of a ferric heme cofactor (Figure S9b, c). No significant changes were observed in the presence or absence of oxidizing or reducing agents under aerobic conditions. However, an increase in the intensity of the absorbance band at ~386 nm and a decrease in absorbance at ~427 nm was observed for CftA upon exposure to the ligands (Figure S9d, e). This spectral shift is consistent with the displacement of heme-bound water by the substrates in a type I mode. 25,26 However, the alpha and beta bands which typically show up at 500~600 nm with this binding mode were too broad to clearly distinguish from the baseline. With our preliminary evidence suggesting that recombinant CftA is cofactor-replete, and its binding site is capable of binding ikarugamycin (1), clifednamide A (2), and C (3), we set out to determine if ikarugamycin (1) is the natural substrate on pathway to clifednamides A (2) and C (3).

P450 monooxygenase CftA converts ikarugamycin (1) to clifednamides A (2) and C (3). Ikarugamycin (1) is the proposed substrate for CftA based on the observation that cftA knockouts result in accumulation of ikarugamycin (1) and loss of clifednamide A (2) and C (3) production. Ikarugamycin (1) is commercially available (Santa Cruz Biotechnology), and before testing it in CftA assays, we validated its purity and identity using LC-MS prior to use (Figure S8). Cytochrome P450 enzymes require the net transfer of two electrons from a reducing source to facilitate oxygen activation by the heme cofactor leading to formation of reactive Fe-oxo intermediates.²⁷ We initially attempted NADH as the sole reductant, which failed to stimulate enzyme turnover by monitoring for clifednamide A (2) production via LC-MS. A survey of the Streptomyces P450 literature revealed that a combination of spinach ferredoxin and spinach ferredoxin reductase can serve as a suitable redox couple to sustain enzyme turnover. ²⁸ Because spinach ferredoxin reductase depends on cost prohibitive NADPH, we employed an NADPH regeneration system using glucose-6-phosphate dehydrogenase to convert D-glucose-6-phosphate and NADP⁺ to 6-phospho-D-glucono-1,5-lactone and NADPH.²⁹ By utilizing this coupled redox system, we were able to achieve CftA-dependent conversion of ikarugamycin (1) to clifednamide A (2) (Figure 4a, S11). We made no attempt to identify native redox partners from Streptomyces sp. JV178. While good conversion of ikarugamycin (1) to clifednamide A (2) was observed after 24 hours, the appearance of clifednamide C (3) was delayed and accumulated after 96 hours in single-pot reactions. CftA reactions starting with pure clifednamide A (2) as substrate produced only trace clifednamide C (3), which is consistent with the previous result (Figure S10, S12). We hypothesize that the initial oxidation of ikarugamycin (1) to clifednamide A (2) is fast and subsequent oxidation of clifednamide A (2) to clifednamide C (3) is slow.

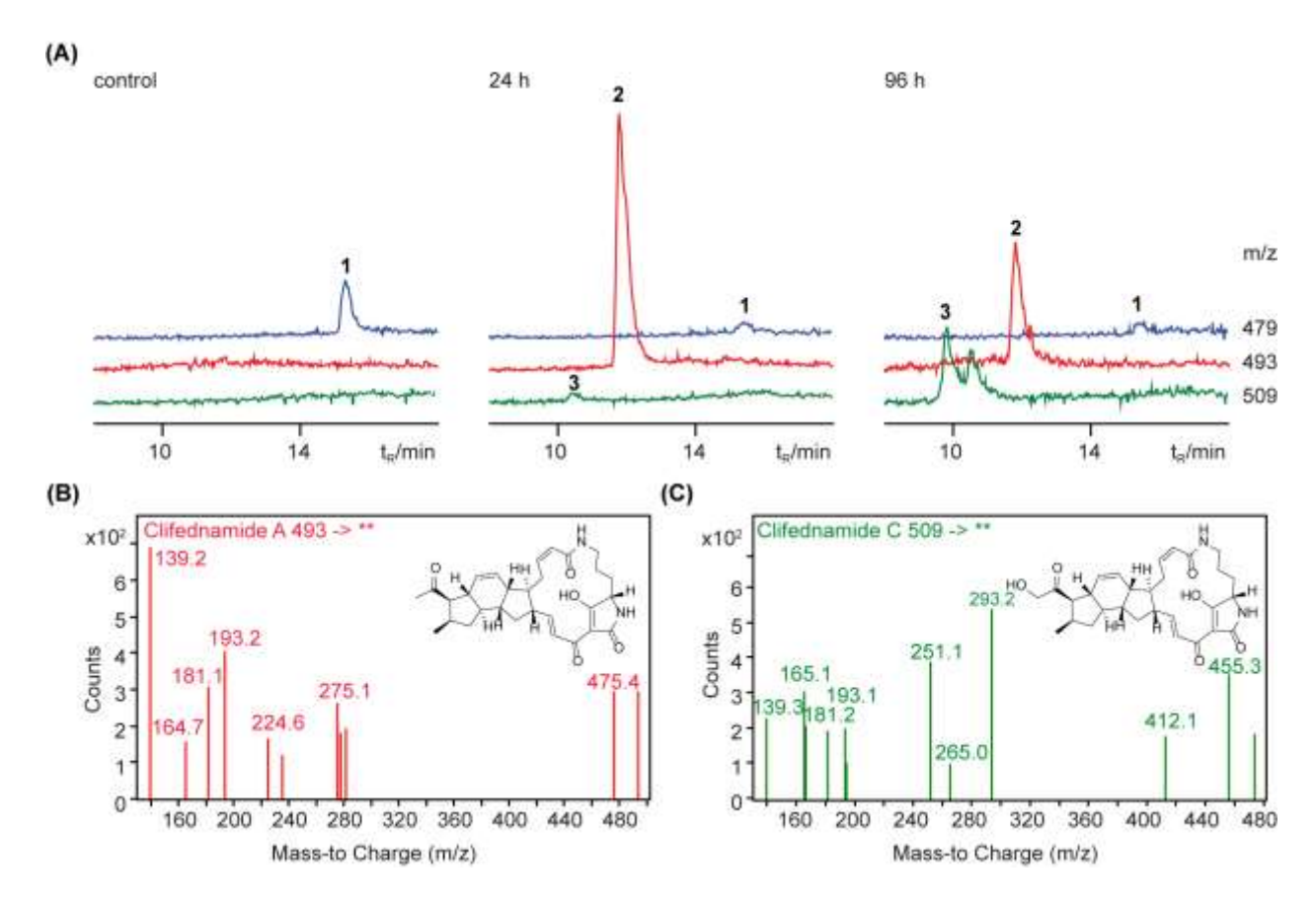


Figure 4. *In vitro* reconstitution of CftA activity demonstrating site selective C-H oxidation of ikarugamycin (1) to produce clifednamides A (2) and C (3). (a) Extracted ion chromatograms (EICs) generated from low resolution single quadrupole LC-MS analyses of CftA reaction mixtures after 24 h and 96 h. Control reaction contains no CftA. The *m/z* values correspond to [M+H]⁺ molecular ions for ikarugamycin (1, 479), clifednamide A (2, 493), and clifednamide C (3, 509). The x-axis represents retention time (t_R). The y-axis represents relative EICs for target ions. Panels (b) and (c) show triple quadrupole MS-MS analyses of the [M+H]⁺ molecular ions for (b) clifednamide A (2) and (c) clifednamide C (3).

We confirmed the bond connectivity of clifednamide A (2) and C (3) generated via CftA *in* vitro CftA via mass fragmentation using tandem MS/MS analysis (Figure 4b, c). The MS/MS spectra recorded show common molecular fragments derived from the 'right-hand' ornithine tetramate moiety (m/z = 139, 181), consistent with previous reports of MS/MS analysis of PTMs.⁸

The fragmentation patterns for the 'left-hand' polycyclic portion of the molecules are unique between different PTMs, and those that we found are consistent with CftA-catalyzed C-H oxygen insertion at methyl C30 as determined by multi-dimensional NMR characterization of clifednamide C (3) derived from *Streptomyces* culture (Figure 3). As the MS/MS fragmentation patterns for *in vitro* produced clifednamide C (3) are identical to the ones previously reported by the Blodgett group from growth extracts, 8 we propose that the bond connectivity of clifednamide C (3) derived from ikarugamycin (1) in the CftA in vitro reaction is the same as clifednamide C (3) isolated from *Streptomyces* culture. However, we did unexpectedly observe two molecular ion peaks corresponding to the expected [M+H]⁺ ion for clifednamide C (3) suggesting the presence of isomers. These putative isomers generated a similar profile of daughter [M+H] ions in the MS/MS fragmentation patterns (Figures 4c and S13). Interestingly, ikarugamycin (1) has two naturally occurring isomers, ikarugamycin (1) and iso-ikarugamycin, differing only in the location of an olefin at either C2-C3 or C3-C4, respectively.³⁰ Additionally, the combamides are related PTM natural products where there is an alpha-hydroxy-ketone at C29-C11 in combamide A instead of the hydroxymethyl ketone at C29-C30 for clifednamide C (3).⁴ While we did not find evidence for these isomers in our NMR characterization of pure clifednamide C (3) from Streptomyces culture, it is possible that in vitro CftA-reaction conditions with commercially available ikarugamycin (1) might lead to clifednamide C (3) isomers structurally related to either isoikarugamycin or combamide A (Figure S14).

CftA shares an evolutionary relationship to multi-functional P450 enzymes. Inspired by the structural similarity of clifednamides, combamides, and related PTMs, we generated a maximum likelihood phylogenetic tree for P450s encoded in natural product BGCs including those found in PTM operons (Figure 5a; Table S8). The production of clifednamide C (3) requires saturated C-H

bond hydroxylation and three rounds of oxygen insertion catalyzed by CftA. Thus, to map the functional and evolutionary relationships of CftA we included in our phylogenic analysis a variety of P450 enzymes from natural product biosynthetic pathways that have been associated with hydroxylation via C-H activation on saturated carbon centers, epoxidation of olefins, or dual functions.³¹ We also included cytochrome P450s from *Streptomyces* sp. with similar functions that were compiled in a recent review by the Shen group. 32 As expected, CftA grouped closest to P450s found in BGCs for the PTMs capsimycin (IkaD)¹³ and combamide (CbmD).⁴ CftA shares 46% and 54% sequence identity to IkaD and CbmD, respectively (Table S9). The nearest P450 having a reported structure in the PDB is MycG from the biosynthetic pathway for the mycinamicin family of macrolide antibiotics. 33,34 CftA is 49% sequence identical to MycG. Sequence alignment of CftA, IkaD, CbmD, and MycG reveal conservation of critical residues in the heme binding pocket including the Cys-ligand-loop and L-helix (Figure S15). The most sequence diverse motifs are located in the F- and G-helical regions, which are proposed to be correlated with substrate binding and recognition.³⁵ MycG is a multi-functional P450 that catalyzes sequential tandem oxidations at vicinal atomic sites in the substrate. The orientation of M-IV substrate in the ligand-bound MycG structure reveals close proximity of the allylic system that can undergo C-H bond activation on pathway to hydroxylation, epoxidation, or both to generate oxidized products M-V, M-I, or M-II, respectively (Figure 5b, c). MycG serves as a useful model for CftA since CftA also catalyzes sequential tandem oxidations in the conversion of ikarugamycin (1) to clifednamide A (2) and C (3) as shown in this work (Figure 2). We created a structural homology model of CftA using the SWISS-MODEL software package on the Expasy web server (https://swissmodel.expasy.org/) with the MycG structure in complex with M-V (PDB 5uhu) as the template. 33,36 All major structural elements including the F-, I-, and L-helical bundle that forms the active site and heme

binding motifs were intact and QMEAN scores were in the acceptable range.³⁶ We manually docked ikarugamycin (1) into the CftA model active site using the Cambridge Crystallographic Data Centre (CCDC) coordinates from the small-molecule single crystal X-ray structure (CCDC 1871524)²² to demonstrate the sufficient binding cavity volume needed to orient the C29–C30 ethyl group within striking distance of the heme iron center (Figure 5d). Presumably this type of binding mode would enable the observed sequential oxidations of ikarugamycin (1) to clifednamide A (2) and clifednamide A (2) to clifednamide C (3) (Figure 5e).

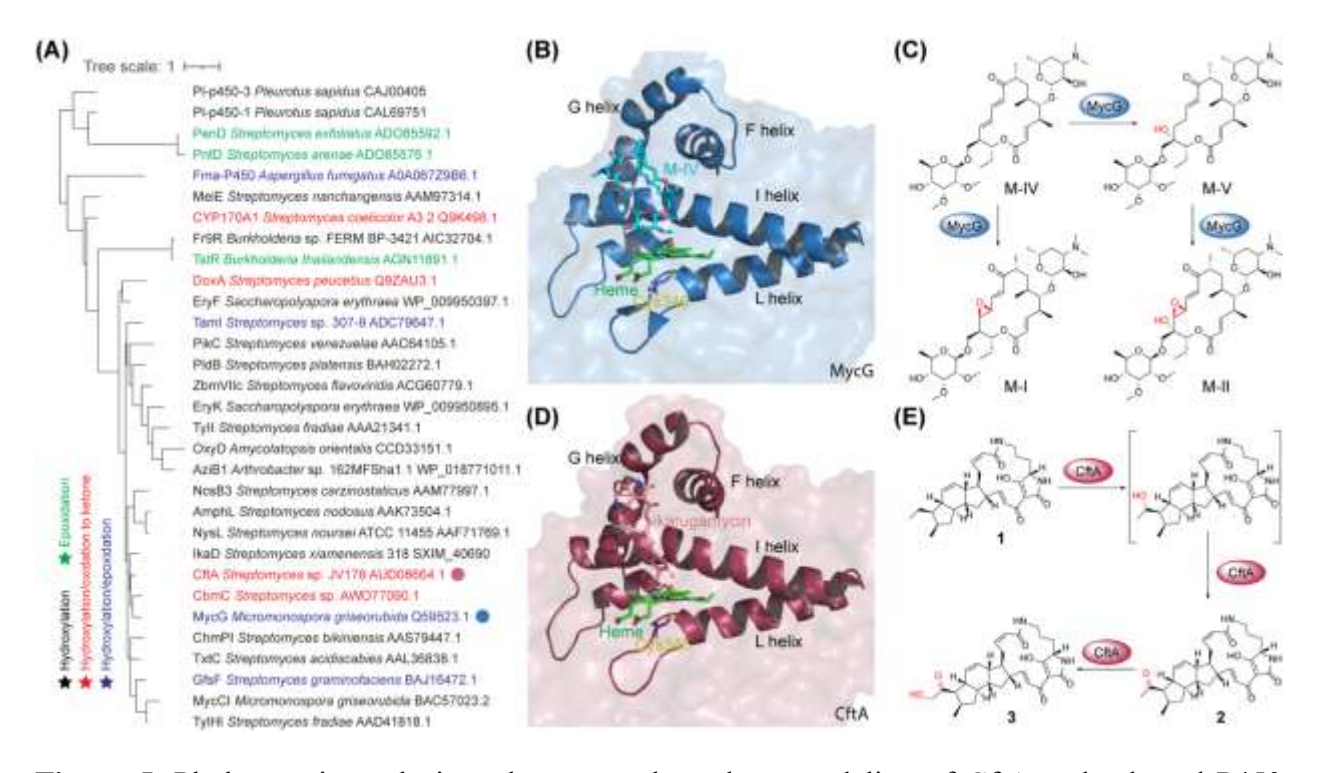


Figure 5. Phylogenetic analysis and structure homology modeling of CftA and selected P450 oxygenases. (a) The maximum likelihood tree of selected epoxidation/hydroxylation/duo function P450 enzymes was built by "One-click" method from http://phylogeny.fr. (b) The active site of MycG in its solution conformation structure (PDB: 5uhu).³³ (c) The last two-step oxidation transforming M-IV to M-II by MycG in the mycinamicin biosynthetic pathway. (d) The active site of CftA generated using SWISS model (https://swissmodel.expasy.org/) with MycG structure (PDB: 5uhu) as template. (e) Proposed oxidation reaction of ikarugamycin (1) catalyze by CftA.

Bioactivity and physiochemical properties of clifednamides. PTMs are known for their antibacterial, antifungal, antiprotozoal, and antitumor activity.³⁷ We tested the antibacterial and antifungal activity of ikarugamycin (1), clifednamide A (2), and C (3) against Bacillus subtilis ATCC 6633, Staphylococcus aureus ATCC 11632, Micrococcus luteus ATCC 10240 and Candida albicans ATCC 48130 using the broth microdilution assay (Table S10). Only ikarugamycin (1) showed growth inhibition towards these microorganisms with apparent MIC₉₀ values in the range of 22.5–45 µM. While the microbial target of PTMs has not been identified, recently, a study by Shu-Heng et al. found that ikarugamycin (1) and capsimycin bind human hexokinase 2 (an isoform absent in bacteria and fungi) and inhibit pancreatic cell glycolysis in vivo.²² Molecular docking studies were used to support a binding mode where the C29–C30 ethyl group of ikarugamycin (1) and C29 methoxy group of capsimycin bind in a buried hydrophobic pocket lined by Val654, Phe602, Cys606, and Asn608. Molecular docking suggests that Cys606 can be oriented near the C29 ketone of clifednamide A and C (3-4 Å from Cys thiolate to C29) with proper trajectory for nucleophilic attack by the thiolate leading to covalent thioketal bond formation (Figure S14). In fact, clifednamides A (2) and B were shown to have potent cytotoxicity against MIA-PaCa2 and A549 cells.¹⁸ The C29–C30 positions do seem to tolerate substitution in the PTM compound class. 18,22,37 Presumably, hydroxylation at C30 in clifednamide C (3) could enable further stabilizing interactions via hydrogen bonding with Asn608, although the antitumor properties of this PTM have not been determined. Tailoring oxidations of PTMs decrease the hydrophobicity (Table S11)³⁸ and may influence the cell penetrating properties of these natural products.^{39,40} Semisynthetic modifications of natural products, including late-stage oxidations, in pharmaceutical discovery programs is often aimed at improving drug-like properties including greater water solubility. 15,16,40,41 Presumably, natural product producing microbes employ

biosynthetic strategies for late-stage oxidation to diversify the metabolic pool, expand/enhance the bioactivity profile, and counteract resistance strategies employed by competing microbes and target organisms. 42,43

Significance

Synthetic access to PTMs is improving but remains challenging due to the structural complexity of this natural product class. ^{19,44,45} Accordingly, microorganismal sources of PTMs for discovery, characterization and bio-combinatorial production remain productive and important. Late-stage oxidation in PTM biosynthesis is used by producing microbes to diversify the product pool and improve water solubility in natural environments. Application of enzymatic site-selective late-stage oxidation of PTMs is an attractive strategy to increase compound potency, install functional group handles, and improve drug-like properties of lead molecules. Functional validation and *in vitro* reconstitution of CftA multi-functional activity opens the door to the application and engineering of this P450 oxidase for targeted applications in PTM late-stage oxidation via site-selective C–H bond activation to support compound discovery and lead optimization efforts for this important class of natural products.

Experimental Section

General Experimental Procedures. All enzymes, cofactors, buffers, and reagents were purchased from Sigma Aldrich (St. Louis, MO) unless otherwise stated. Codon-optimized *cftA* was purchased from GenScript in a pET28a vector for heterologous expression in *E. coli* BL21(DE3) with an *N*-terminal hexahistidine tag. DNA purification was performed with Monach® plasmid miniprep kit. Plasmid sequencing was performed by Genewiz. Nickel-nitriloacetic acid (Ni-NTA)

agarose was purchased from ThermoFisher Scientific. Any kD SDS-PAGE gels were purchased from Bio-Rad. 10K MWCO SnakeSkin dialysis tubing for protein dialysis was purchased from ThermoFisher Scientific. Proteins were concentrated by centrifugal filtration using 30K MWCO filters from Millipore. All aqueous solutions were prepared with water purified using a Milli-Q system. Media was sterilized using an autoclave unless otherwise stated. An Orion Star A111 pH meter was used for pH measurements. All buffers, salts, media, solvent, and chemical reagents were purchased from Sigma Aldrich unless otherwise stated. DNA and protein concentrations were determined using a NanoDrop 2000 UV-Vis spectrophotometer from ThermoFisher Scientific. Protein extinction coefficients were calculated using the ExPasy ProtParam tool. 46 UV-vis optical absorbance spectrophotometry was performed in 1 cm quartz cuvettes on an Agilent Cary 60 spectrophotometer. Optical rotation was recorded on an Autopol III automatic polarimeter. ECD data were collected by a Jasco J-815 Circular Dichroism spectrometer. HRESIMS spectra were obtained by using Ultra-High resolution QTOF MS Bruker maXis II 4G in the positive-ion mode. NMR spectra were recorded on a Varian Unity Inova-600 MHz instrument with a cryo-probe.

Low-resolution LC-MS analyses were performed using an Agilent 6130 quadrupole with G1313 autosampler, G1315 diode array detector, 1200 series solvent module and Phenomenex Gemini C18 column (50 x 2 mm), 5 μ m with guard column. Samples were prepared in 0.45 μ PTEE mini-UniPrep vials from Agilent. Mobile phases were 0.1% formic acid in (A) H₂O and (B) acetonitrile. LC-MS data were processed using G2710 ChemStation software. MS/MS analyses were performed using an Agilent 6420 Triple-Quad mass spectrometer with a 1260 Infinity HPLC module. Separations were achieved using a Phenomenex Luna C18 column (75 Å, ~3 mm, 3 μ m pore size). Mobile phases were 0.1% formic acid in (A) H₂O and (B) acetonitrile with a flow rate of 0.9 mL/min and injection volume of 10 μ L per run. Molecular [M+H]⁺ ions of interest were

identified using precursor ion scan mode with fragmentation into daughter [M+H]⁺ ions with m/z values of 139.2. MS/MS data were processed using Agilent MassHunter Qualitative Analysis software. Preparative HPLC was performed using an Agilent/HP 1050 quaternary pump module and Agilent/HP 1050 MWD detector with a Phenomenex Luna 10 μ C18(2) 100 Å column, 250 x 21.20 mm, 10 μ m with guard column. Mobile phases were 0.1% formic acid in (A) H₂O and (B) acetonitrile. HPLC data were processed using ChemStation software.

Microbial Strains. *Streptomyces* sp. strain NRRL F-2890 JV772 was developed by the Blodgett lab for enhanced heterologous production of clifednamide A (2) and C (3).⁸ *E. coli* BL21-Gold (DE3) was obtained from Agilent and used as the host for plasmid construction and protein expression.

Fermentation, extraction, and purification of clifednamides A and C. Genetically engineered strain *Streptomyces sp.* strain NRRL F-2890 JV772 was pre-cultured in 5 mL aliquots of tryptic soy broth liquid medium in 14 mL culture tubes with shaking (225 r.p.m.) at 28°C under aerobic conditions. Two 6-mm glass beads were added to each tube to disrupt mycelial clumps during growth incubation. After 2 days of growth, 200 μL of the pre-cultures were plated on ATCC 172 agar plates (10 g/L glucose, 20 g/L soluble starch, 5 g/L yeast extract, 5 g/L N-Z amine type A, 1 g/L reagent grade CaCO₃, 15 g/L agar) and incubated at 28 °C for 6 days under aerobic conditions. The agar was diced and extracted with 30 mL of EtOAc per plate. The EtOAc solution was then removed via rotary evaporation under reduced pressure. The resulting crude extract was suspended in HPLC-grade MeOH and passed through a 0.2 μ syringe filter to afford a ~5 mg/mL solution for purification via RP-C18 pre-HPLC. Separation was achieved using a gradient of 0–5% B over 1 min, 5–60% over 12 min, 60-100% B over 10 min, and hold at 100% B for 3 min with a flow rate of 9 mL/min on 2 mL injections of the ~5 mg/mL stock solution of crude extract in

MeOH. Fractions containing clifednamide A (2; 17.6 min) and clifednamide C (3; 14.9 min) were collected based on characteristic optical absorbance peaks monitored at $\lambda = 320$ nm and were confirmed via LC-MS analysis (Figure S3) and characterized via multi-dimensional NMR (Figures S17–S25).

Clifednamide C (3): light pink, amorphous powder; $[\alpha]_D^{20}$ +23 (c 0.36, DMSO); UV (MeOH) λ_{max} (log ϵ) 292 (4.02), 324 (3.94), 397 (3.31) nm; ECD (0.54 mM, MeOH), λ_{max} ($\Delta\epsilon$) 248 (-24.07), 326 (11.71) nm; ¹H and ¹³C NMR, Table S12; HRESIMS m/z 509.2630 [M + H]+ (calcd for $C_{29}H_{37}N_2O_6^+$, 509.2646).

Cloning, expression, and purification of CftA P450 oxygenase. Codon-optimized cftA was purchased from GenScript and cloned into a pET28a expression plasmid (Table S6). The pET28acftA plasmid was transformed into E. coli BL21 (DE3) for plasmid amplification and protein expression purposes. Cells harboring the plasmid were first grown at 37 °C overnight in LB broth containing 50 µg/mL kanamycin as the selection antibiotic. The overnight cell culture was then used to inoculate 1 L of terrific broth (24 g/L yeast extract, 12 g/L tryptone, 5 g/L glycerol, 17 mM KH₂PO₄, 72 mM K₂HPO₄) containing 50 μg/mL kanamycin in a 2.8 L baffled flask. The culture was shaken at 37 °C until an OD_{600} of approximately ~0.5 was reached. The cells were cold shocked in ice bath and protein expression was induced by the addition of 0.5 mM isopropyl β-D-1-thiogalactopyranoside (final concentration). The induced cell culture was then incubated overnight with agitation (225 r.p.m.) at 20 °C. Cells were harvested by centrifugation at 5,000 r.p.m. for 30 min at 4 °C. Cell pellets were resuspended in 40 mL of lysis buffer (50 mM Tris-HCl, 500 mM NaCl, and 25 mM imidazole pH 8.0). The resulting cell suspension was flash frozen in liquid nitrogen and stored at -80 °C. Cells were thawed and gently rocked for 30 min at 4 °C before mechanically lysed by passing through an Avestin EmulsiFlex-C5 cell disruptor. The cell lysates

were clarified by centrifugation at 45,000 r.p.m. for 35 min at 4 °C. The resulting yellow supernatant was incubated with Ni-NTA resin in lysis buffer for 30 min at 4 °C in a fritted glass column. The Ni-NTA resin was washed three times with five column volume of lysis buffer (50 mM HEPES, 500 mM NaCl, and 50 mM imidazole, pH 8.0). After washing, protein was eluted with 50 mL of elution buffer (50 mM HEPES, 500 mM NaCl, and 500 mM imidazole, pH 8.0). The elution fractions were analyzed by SDS-PAGE (Figure S9a). Fractions containing pure CftA (>95%) were combined, dialyzed overnight in dialysis buffer (50 mM HEPES, pH 8.0) and concentrated using a 30 K MWCO Amicon centrifugal filter.

Optical absorbance measurements of CftA. Optical absorbance spectra were recorded using an Agilent Cary 50 UV-vis spectrophotometer with an optical window from $\lambda = 300 - 800$ nm in a 1 cm quartz micro-cuvette. CftA protein solution was diluted to 60 μ M in 100 mM potassium phosphate buffer, pH 7. Changes in absorbance bands were monitored in the presence of oxidant or reductant. A 100 μ L solution of 60 μ M CftA was mixed with either 100 μ L of 600 μ M m-CPBA or 100 μ L of 600 μ M prior to analysis. For substrate binding studies, 75 μ L of 60 μ M CftA was mixed with 75 μ L of 100 mM potassium phosphate buffer and 10 μ L of ligand (ikarugamycin (1), clifednamide A (2), or clifednamide C (3)) at 2.16 mM. All spectra were recorded within 1 min after sample mixing (Figure S9b, c, d).

In vitro reconstitution of CftA activity. Reactions were prepared in 100 mM TAPS buffer (pH 8.0) with 50 μM ikarugamycin (1) or clifednamide A (2), 25 μM CftA, 0.1 U/mL ferredoxin-NADP+ reductase, 32 μg/mL spinach ferredoxin and an NADPH-regeneration system consisting of 40 mM glucose-6-phosphate, 4 mM NADP+, 1 mM MgCl₂, 4 U/mL glucose-6-phosphate dehydrogenase. The NADPH-regeneration system was incubated at 37 °C for 30 min to generate a saturated pool of NADPH before initiating reactions. Reactions were initiated by addition of

CftA and were incubated at room temperature with gentle agitation. After 24 h and 96 h, aliquots of the reaction mixture were quenched with an equal volume of methanol. The quenched samples were centrifuged at 14,800 r.p.m. for 2 min to pellet the precipitated protein and the supernatant was syringe-filtered prior to analysis by LC-MS.

Phylogenetic and homology modeling of CftA. A selection of protein sequences representing P450 oxygenases that catalyze a variety of oxidative transformations (epoxidation, hydroxylation, and multi-functional oxidations) were compiled based on functional reports in the primary literature (Table S9). Amino acid sequences were downloaded from the NCBI database (https://www.ncbi.nlm.nih.gov/). Phylogenetic analysis was performed by using 'One Click' method from Phylogeny.fr.⁴⁷ The phylogenetic tree was visualized and annotated using iTOL v6 (Figure 5a).⁴⁸ Sequence alignments of MycG, CbmD, IkaD, and CftA were performed using the Clustal Omega online tool from EMBL (Figure S15).⁴⁹ The alignment result was viewed in M-view and the secondary structure was denoted manually based on the solution conformation of cytochrome P450 MycG with M-IV bound (PDB:5uhu). A CftA homology model was built using SWISS–MODEL with MycG (PDB: 5uhu) as template (Figures 2 and 5d).³⁶ The 3D structure of ikarugamycin (1) used in the docking study was obtained from the Cambridge Crystallographic Data Centre (CCDC 1871524). Ikarugamycin (1) was manually docked to minimize steric interactions using the M-IV substrate in the MycG template structure as a guide.

Antibacterial susceptibility testing. The antibacterial activities of ikarugamycin (1), clifednamide A (2), and clifednamide C (3) against *Bacillus subtilis* ATCC 6633, *Staphylococcus aureus* ATCC 43300, and *Micrococcus luteus* ATCC 10240 were evaluated using the broth microdilution assay following Clinical and Laboratory Standards Institute (CLSI) guidelines in Mueller-Hinton No. 2 (MHII) broth (Table S10). Minimal inhibitory concentrations (MIC₉₀ values)

were judged visually as the concentration of compound resulting in reduction of ~90% of cellular growth. Each well of a 96-well plate was filled with 50 µL of sterile MHII broth. A 50 µL aliquot of test compound at 720 µM in water was added to the first row of 96-well plate and diluted 2-fold down the plate to afford a concentration gradient of 360, 180, 90, 45, 22.5, 11.2, 5.6 and 2.8 µM test compounds. A 50 μL cell suspension of inoculum (~10⁶ cfu/mL in MHII broth) was added to each well to provide a final working volume of 100 µL per well. A concentration gradient of 1250, 625, 312.5, 156.3, 78.1, 39.1, 19.5, 9.8, 4.9, and 2.4 µg/mL ampicillin was also applied to the tested bacteria as a positive control. Microwell plates were incubated at 37 °C for 18 h before judging the MIC₉₀ breakpoints. The antifungal microbroth dilution assay against *Candida albicans* ATCC 48130 was performed analogously except for using RPMI 1640 media in the test and yeast inoculum suspension.⁵⁰ Briefly, yeasts were first grown on Sabouraud dextrose agar (40 g/L dextrose, 10 g/L peptone and 15 g/L agar in water) for 24 h. The inoculum suspension was prepared by picking single colonies (at least 1mm in diameter) and suspending the materials in 5 mL of 0.85% saline. The suspension was diluted to A530 = 0.125 and subsequently further diluted 50fold in RPMI 1640 medium to yield a final inoculum concentration of approximately 0.2 x 10⁵ to 1×10^5 cfu/mL.

ASSOCIATED CONTENT

The Supporting Information is available free of charge online at https://pubs.acs.org/journal/jnprdf.

Supporting figures, supporting tables, compound characterization data, compound purity analyses, MS-MS spectra, LC-MS chromatograms, NMR spectra, optical absorbance spectra, protein purity analysis, protein sequence alignments.

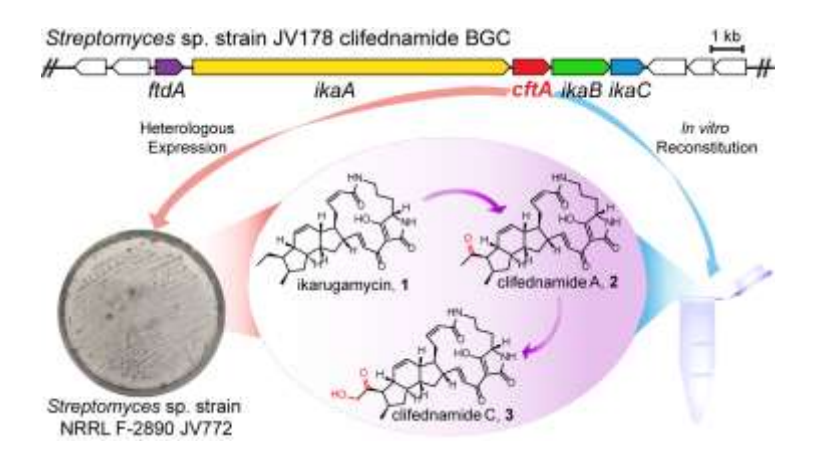
NOTES

The authors declare no competing financial interest.

ACKNOWLEDGMENTS

The authors would like to thank Drs. Jeff Kao and Manmilan Singh (WUSTL Chemistry) for help with the acquisition of 2D NMR data. The authors thank Spencer Stumpf and Keshav K. Nepal (WUSTL Biology) for assistance with strain growth and acquisition of LC-MS/MS data. The authors also thank Dr. Deanna Mendez for the assistance with the CD spectroscopy experiments. High-resolution mass spectrometry experiments in this study made use of the NIH/NIGMS Biomedical Mass Spectrometry Resource at Washington University in St. Louis, MO, which is supported in part by the National Institute of General Medical Science within the National Institutes of Health through 5P41GM103422. Funding for this work was provided in part by the Sloan Foundation, Research Corporation for Science Advancement, and the Camille and Henry Dreyfus Foundation through Sloan Fellowship, Cottrell Scholar Award, and Camille Dreyfus Teacher Scholar Award to T. A. W. This work was also partially supported by the National Science Foundation under NSF-CAREER awards 1846005 to J. A. V. B. and 1654611 to T. A. W.

FOR TABLE OF CONTENTS USE ONLY



AUTHOR INFORMATION

Corresponding Authors

Timothy A. Wencewicz – Department of Chemistry, Washington University in St. Louis, St. Louis, MO, 63130, USA;

orcid.org/0000-0002-5839-6672; Email: wencewicz@wustl.edu

Joshua A. V. Blodgett - Department of Biology, Washington University in St. Louis, One Brookings Drive, St. Louis, MO, 63130, USA;

orcid.org/0000-0002-7080-5870; Email: jblodgett@wustl.edu

Authors

Jinping Yang - Department of Chemistry, Washington University in St. Louis, St. Louis, MO, 63130, USA;

orcid.org/0000-0002-9791-4751

Yunci Qi - Department of Biology, Washington University in St. Louis, One Brookings Drive, St. Louis, MO, 63130, USA;

orcid.org/0000-0002-0150-1777

Author Contributions

J.Y., J.A.V.B, and T.A.W. designed the experiments and wrote the manuscript. J.Y. and Y.Q. performed experiments.

Notes

The authors declare no competing financial interest.

REFERENCES

- (1) Blodgett, J. A. V.; Oh, D. C.; Cao, S.; Currie, C. R.; Kolter, R.; Clardy, J. *Proc. Natl. Acad. Sci. U. S. A.* **2010**, *107*, 11692–11697.
- (2) Zhang, G.; Zhang, W.; Saha, S.; Zhang, C. Curr. Top. Med. Chem. 2015, 16, 1727–1739.
- (3) Jomon, K.; Kuroda, Y.; Ajisaka, M.; Sakai, H. J. Antibiot. (Tokyo). 1972, 25, 271–280.
- (4) Liu, Y.; Wang, H.; Song, R.; Chen, J.; Li, T.; Li, Y.; Du, L.; Shen, Y. *Org. Lett.* **2018**, *20*, 3504–3508.
- (5) Yu, F.; Zaleta-Rivera, K.; Zhu, X.; Huffman, J.; Millet, J. C.; Harris, S. D.; Yuen, G.; Li, X. C.; Du, L. *Antimicrob. Agents Chemother.* **2007**, *51*, 64–72.
- (6) Lou, L.; Qian, G.; Xie, Y.; Hang, J.; Chen, H.; Zaleta-Rivera, K.; Li, Y.; Shen, Y.; Dussault, P. H.; Liu, F.; Du, L. J. Am. Chem. Soc. 2011, 133, 643–645.
- (7) Fisch, K. M. *RSC Adv.* **2013**, *3*, 18228–18247.
- (8) Qi, Y.; Ding, E.; Blodgett, J. A. V. ACS Synth. Biol. **2018**, 7, 357–362.
- (9) Saha, S.; Zhang, W.; Zhang, G.; Zhu, Y.; Chen, Y.; Liu, W.; Yuan, C.; Zhang, Q.; Zhang,
 H.; Zhang, L.; Zhang, W.; Zhang, C. *Chem. Sci.* 2017, 8, 1607–1612.
- (10) Luo, Y.; Huang, H.; Liang, J.; Wang, M.; Lu, L.; Shao, Z.; Cobb, R. E.; Zhao, H. *Nat. Commun.* **2013**, *4*.
- (11) Li, Y.; Huffman, J.; Li, Y.; Du, L.; Shen, Y. *Medchemcomm* **2012**, *3*, 982–986.

- (12) Greunke, C.; Antosch, J.; Gulder, T. A. M. Chem. Commun 2015, 5334, 5334.
- (13) Yu, H. L.; Jiang, S. H.; Bu, X. L.; Wang, J. H.; Weng, J. Y.; Yang, X. M.; He, K. Y.; Zhang, Z. G.; Ao, P.; Xu, J.; Xu, M. J. *Sci. Rep.* **2017**, *7*.
- (14) Yan, Y.; Wang, H.; Song, Y.; Zhu, D.; Shen, Y.; Li, Y. ACS Synth. Biol. **2021**, 10, 2434–2439.
- (15) Hong, B.; Luo, T.; Lei, X. ACS Cent. Sci. 2020, 6, 622–635.
- (16) Fessner, N. D. ChemCatChem **2019**, 11, 2226–2242.
- (17) Cao, S.; Blodgett, J. A. V.; Clardy, J. Org. Lett. **2010**, 12, 4652–4654.
- (18) Jiao, Y. J.; Liu, Y.; Wang, H. X.; Zhu, D. Y.; Shen, Y. M.; Li, Y. Y. J. Nat. Prod. **2020**, 83, 2803–2808.
- (19) Sinast, M.; Claasen, B.; Stöckl, Y.; Greulich, A.; Zens, A.; Baro, A.; Laschat, S. *J. Org. Chem.* **2021**, *86*, 7537–7551.
- (20) Dhaneesha, M.; Hasin, O.; Sivakumar, K. C.; Ravinesh, R.; Naman, C. B.; Carmeli, S.; Sajeevan, T. P. *Mar. Biotechnol.* **2019**, *21*, 124–137.
- (21) Qi, Y.; D'Alessandro, J. M.; Blodgett, J. A. V. Genome Announc. 2018, 6.
- (22) Jiang, S. H.; Dong, F. Y.; Da, L. T.; Yang, X. M.; Wang, X. X.; Weng, J. Y.; Feng, L.; Zhu, L. L.; Zhang, Y. L.; Zhang, Z. G.; Sun, Y. W.; Li, J.; Xu, M. J. FASEB J. 2020, 34, 3943–3955.
- (23) Murphy, S. K.; Zeng, M.; Herzon, S. B. Science (80-.). 2017, 356, 956–959.
- (24) Yamanoi, T.; Oda, Y.; Katsuraya, K.; Inazu, T.; Hattori, K. *Bioorganic Med. Chem.* **2016**, *24*, 635–642.
- (25) Mak, P. J.; Denisov, I. G. Biochim. Biophys. Acta Proteins Proteomics 2018, 1866, 178–204.
- (26) Isin, E. M.; Guengerich, F. P. Anal. Bioanal. Chem. 2008, 392, 1019–1030.
- (27) Meunier, B.; de Visser, S. P.; Shaik, S. Chem. Rev. 2004, 104, 3947–3980.
- (28) Hannemann, F.; Bichet, A.; Ewen, K. M.; Bernhardt, R. *Biochim. Biophys. Acta Gen. Subj.* **2007**, *1770*, 330–344.

- (29) Han, S.; Pham, T. V.; Kim, J. H.; Lim, Y. R.; Park, H. G.; Cha, G. S.; Yun, C. H.; Chun, Y. J.; Kang, L. W.; Kim, D. *Arch. Biochem. Biophys.* **2015**, *575*, 1–7.
- (30) Lacret, R.; Oves-Costales, D.; Gómez, C.; Díaz, C.; De La Cruz, M.; Pérez-Victoria, I.; Vicente, F.; Genilloud, O.; Reyes, F. *Mar. Drugs* **2015**, *13*, 128–140.
- (31) Liu, X. Synth. Syst. Biotechnol. **2016**, 1, 95–108.
- (32) Rudolf, J. D.; Chang, C. Y.; Ma, M.; Shen, B. Nat. Prod. Rep. 2017, 34, 1141–1172.
- (33) Tietz, D. R.; Podust, L. M.; Sherman, D. H.; Pochapsky, T. C. *Biochemistry* **2017**, *56*, 2701–2714.
- (34) Li, S.; Tietz, D. R.; Rutaganira, F. U.; Kells, P. M.; Anzai, Y.; Kato, F.; Pochapsky, T. C.; Sherman, D. H.; Podust, L. M. *J. Biol. Chem.* **2012**, *287*, 37880–37890.
- (35) Pochapsky, T. C.; Kazanis, S.; Dang, M. *Antioxidants Redox Signal.* **2010**, *13*, 1273–1296.
- (36) Waterhouse, A.; Bertoni, M.; Bienert, S.; Studer, G.; Tauriello, G.; Gumienny, R.; Heer, F. T.; De Beer, T. A. P.; Rempfer, C.; Bordoli, L.; Lepore, R.; Schwede, T. *Nucleic Acids Res.* 2018, 46, W296–W303.
- (37) Jiang, M.; Chen, S.; Li, J.; Liu, L. *Mar. Drugs* **2020**, *18*.
- (38) Ertl, D. P. Calculation of Molecular Properties and Bioactivity score © Molinspiration Cheminformatics https://www.molinspiration.com/cgi-bin/properties (accessed 2021 -06 20).
- (39) O'Shea, R.; Moser, H. E. J. Med. Chem. **2008**, *51*, 2871–2878.
- (40) Richter, M. F.; Drown, B. S.; Riley, A. P.; Garcia, A.; Shirai, T.; Svec, R. L.; Hergenrother, P. J. *Nature* **2017**, *545*, 299–304.
- (41) Lamarche, M. J.; Leeds, J. A.; Amaral, A.; Brewer, J. T.; Bushell, S. M.; Deng, G.; Dewhurst, J. M.; Ding, J.; Dzink-Fox, J.; Gamber, G.; Jain, A.; Lee, K.; Lee, L.; Lister, T.; McKenney, D.; Mullin, S.; Osborne, C.; Palestrant, D.; Patane, M. A.; Rann, E. M.; Sachdeva, M.; Shao, J.; Tiamfook, S.; Trzasko, A.; Whitehead, L.; Yifru, A.; Yu, D.; Yan, W.; Zhu, Q. *J. Med. Chem.* **2012**, *55*, 2376–2387.

- (42) Wencewicz, T. A. J. Mol. Biol. 2019, 431, 3370–3399.
- (43) Wencewicz, T. A. Bioorganic Med. Chem. 2016, 24, 6227–6252.
- (44) Loke, I.; Bentzinger, G.; Holz, J.; Raja, A.; Bhasin, A.; Sasse, F.; Köhn, A.; Schobert, R.; Laschat, S. *Org. Biomol. Chem.* **2016**, *14*, 884–894.
- (45) Bodenschatz, K.; Stöckl, J.; Winterer, M.; Schobert, R. Tetrahedron 2021, 132113.
- (46) Artimo, P.; Jonnalagedda, M.; Arnold, K.; Baratin, D.; Csardi, G.; De Castro, E.; Duvaud, S.; Flegel, V.; Fortier, A.; Gasteiger, E.; Grosdidier, A.; Hernandez, C.; Ioannidis, V.; Kuznetsov, D.; Liechti, R.; Moretti, S.; Mostaguir, K.; Redaschi, N.; Rossier, G.; Xenarios, I.; Stockinger, H. *Nucleic Acids Res.* **2012**, *40*.
- (47) Dereeper, A.; Guignon, V.; Blanc, G.; Audic, S.; Buffet, S.; Chevenet, F.; Dufayard, J. F.; Guindon, S.; Lefort, V.; Lescot, M.; Claverie, J. M.; Gascuel, O. *Nucleic Acids Res.* **2008**, *36*.
- (48) Letunic, I.; Bork, P. *Bioinformatics* **2007**, *23*, 127–128.
- (49) McWilliam, H.; Li, W.; Uludag, M.; Squizzato, S.; Park, Y. M.; Buso, N.; Cowley, A. P.; Lopez, R. *Nucleic Acids Res.* **2013**, *41*.
- (50) Anaissie, E. J.; Paetznick, V. L.; Ensign, L. G.; Espinel-Ingroff, A.; Galgiani, J. N.; Hitchcock, C. A.; Larocco, M.; Patterson, T.; Pfaller, M. A.; Rex, J. H.; Rinaldi, M. G. Antimicrob. Agents Chemother. 1996, 40, 2387–2391.